Development of dual crosslinked mumio-based hydrogel dressing for wound healing application: Physico-chemistry and antimicrobial activity

Research Paper

Development of dual crosslinked mumio-based hydrogel patch for wound healing application: Physico-chemistry and antimicrobial activity

Oyunchimeg Zandraa[1,2]*, Fahanwi Asabuwa Ngwabebhoh[1,2], Rahul Patwa[1,2], Hau Trung Nguyen[1], Marjan Motiei[1], Nabanita Saha[1,2,3], Tomas Saha[2], Petr Saha[1,2,3]

[1]*Centre of Polymer Systems, University Institute, Tomas Bata University in Zlin, Tr. T. Bati 5678, 76001, Zlin, Czech Republic*

[2]*Footwear Research Centre, University Institute, Tomas Bata University in Zlin, Nad Ovcirnou IV, 3685, Zlin, Czech Republic*

[3]*Faculty of Technology, Tomas Bata University in Zlin, Vavrečkova 275, 76001 Zlin, Czech Republic*

ABSTRACT

In this study, an antimicrobial mumio-based hydrogel dressing was developed for wound healing application. The mechanism of gel formation was achieved via a double crosslink network formation between gelatin (GT) and polyvinyl alcohol (PVA) using polyethylene glycol diglycidyl ether (PEGDE) and borax as crosslinking agents. To enhance the mechanical integrity of the hydrogel matrix, bacterial cellulose (BC) was integrated into the GT-PVA hydrogel to produce a composite gel dressing. The obtained hydrogel was characterized by FTIR, SEM, TGA, and XRD. Gel fraction, *in vitro* swelling and degradation as well as compressive modulus properties of the gel dressing were investigated as a function of change in PVA and BC ratios. By increasing the ratios of PVA and BC, the composite dressing showed lower swelling but higher mechanical strength. Comparing to other formulations, the gel with 4%w/v PVA and 1%w/v BC demonstrated to be most suitable in terms of stability and mechanical properties. *In vitro* cell cytotoxicity by MTT assay on human alveolar basal epithelial (A549) cell lines validated the gels as non-toxic. In addition, the mumio-based gel was compared to other formulations containing different bioactive agents of beeswax and cinnamon oil, which were tested for microbial growth inhibition effects against different bacteria (*S. aureus* and *K. pneumoniae*) and fungi (*C. albicans* and *A. niger*) strains. Results suggested that the gel dressing containing combinations of mumio, beeswax and cinnamon oil possess promising future in the inhibition of microbial infection supporting its application as a suitable patch for wound healing.

Keywords: Hydrogel, Gelatin, Bacterial cellulose, Mumio, Antimicrobial activity

*Corresponding author:
Email address: zandraa@utb.cz (O. Zandraa) and asabuwa@utb.cz (F.A. Ngwabebhoh)

1. Introduction

Hydrogel dressings are widely used in regenerative medicine as drug delivery systems due to their great potential in replacing and rejuvenating any injured or damaged tissues (Chen et al., 2017; Shah et al., 2019). Polymer-based hydrogels are three-dimensional hydrophilic assemblies capable of holding large amounts of water or biological fluids and have attracted great interest among researchers from various disciplines including chemistry, material science and medicine (Erdagi et al., 2020). Till date, several natural and synthetic polymeric hydrogel dressings have been developed using chitosan, gelatin, alginate, collagen, hyaluronic acid, as well as polyvinyl alcohol (PVA) and polyethylene glycol, have been widely utilized for wound healing and tissue regeneration applications (Afshar et al., 2020; Albu et al., 2012; Liu et al., 2020; Shimizu et al., 2014; Yang et al., 2010).

Gelatin (Gel) is a widely use natural polymer and has been applied in the fabrication of various biomaterials attributed to its biological origin, solubility and excellent biocompatible properties (Nikkhah et al., 2016). However, due to the major drawback associated with this polymer such as rapid degradation and poor mechanical properties, hampers its application in tissue engineering (Liu et al., 2019). Thus, it is essential to blend gelatin with other polymers to enhance mechanical integrity, processability and performance of the materials generated thereafter. Bacterial cellulose (BC), an extracellular polysaccharide is biosynthesized by *Komagataeibacter xylinus* bacteria (Chiaoprakobkij et al., 2020). BC is similar in chemical structure to that of cellulose from plants and has been widely investigated in the fabrication of cellulose-based biocomposites as alternative biomedical materials (de Oliveira Barud et al., 2016). This biopolymer behaves as a reinforcing agent or binder in composites thereby enhancing performance and mechanical strength (Cielecka et al., 2018; Tayeb et al., 2018). Until now, BC has been extensively utilized in the form of hydrogels, blends, fiber membranes and porous scaffolds for different biological and clinical applications in biomedicine, including drug delivery, tissue engineering, and wound dressing (Dumanli, 2017; L. Cacicedo et al., 2016; Ngwabebhoh and Yildiz, 2019). However, native BC membrane do not depict antimicrobial activity and show low capability in entrapment and control release of small molecules like antibiotics (Cacicedo et al., 2016). In order to overcome these limitations, controlled release systems are developed by incorporating BC in other crosslinked polymer systems to form interpenetrating polymeric network (IPN) hydrogels that can alter pore

size and interchain strength (Ngwabebhoh et al., 2021). Polyvinyl alcohol (PVA) is a common non-toxic synthetic biodegradable polymer that has been extensively employed in the preparation of hydrogels towards drug delivery applications (Das and Subuddhi, 2019). PVA possesses good thermal and chemical stability, long-term pH, temperature resistance and good biocompatible properties in living tissues (Deshpande et al., 2012). In addition, PVA exhibits minimal protein adsorption and cell adhesion properties. However, pristine PVA gel systems are known to be fragile in nature and are usually crosslinked by the use of crosslinking agents or radiation in the presence of other polymers in order to improve their mechanical integrity (Tao et al., 2019).

As a polymeric based drug delivery carrier system, major drawbacks that are inevitably related with hydrogels is the inefficiency to control the initial burst release of drugs. This initial burst releases have been known to cause negative effects in some patients. In addition, the burst release may be too high leading to loss in both therapeutically and economical efficacy (Huang and Brazel, 2001). Therefore, by crosslinking this results in elasticity of the carrier matrix and decreases solubility as well as viscosity of the polymer, which provides strength and toughness material developed (Maitra and Shukla, 2014). Different crosslinking techniques have been widely applied, which can be physically crosslinked by UV-radiation and hydrogen bond interaction or chemical crosslinking using aldehydes (e.g., glutaraldehyde and formaldehyde), carbodimides, polyepoxy compounds (polyethylene glycol diglycidyl ether (PEDGE)), etc. (Erdagi et al., 2020; Han et al., 2014; Vargas et al., 2008).

Wound dressing hydrogels reduce pain, ensure bacteria entrapment and provides protecting lesion from bacterial infections. To further strengthen their protection ability against bacteria, bioactive agents such as plant essential oils (EO) have been used and proven to be a long-term friendly alternative, replacing conventional preservatives and antibacterial agent (Gherman et al., 2018). For centuries, essential oils have been used as vital ingredients in cosmetic and health care products and have demonstrated to possess a wide spectrum of antimicrobial activity (Schmitt et al., 2010). Common essential oil extracts of cinnamon, clove, tea tree, eucalyptus, peppermint, sea buckthorn and a few others have been reported to show anti-inflammatory, antioxidant, anticancer and antimicrobial effects against as dermatology related disorders (Miguel, 2010; Tsai et al., 2011). Mumio, also known as mumijo or shilajit is a widely used traditional medicine, especially in Russia, Mongolia, Iran, Kazakhstan and Kyrgyzstan (Aiello et al., 2011;

Sukhdolgor and Orkhonselenge, 2011). It is a thick, sticky tar-like substance and mainly found in rock crevices at altitudes of 2000 to 5000 meters high in mountainous regions of Asia and Antarctica (Garedew et al., 2004; Zandraa et al., 2011). Generally, Mumio contains about 14–20% moisture, 18–20% minerals; 13–17% proteins; 4–4.5% lipids; 3.3–6.5% steroids, 18–20% nitrogen-free compounds, 1.5–2% carbohydrates, and 0.05–0.08% alkaloids, amino acids and other compounds with nitrogen, essentials oils and vitamins etc (Konstantinov et al., 2013). This traditional medicine has proven to possess a wide spectrum of pharmacological activity and in combination with honey has been prescribed as an antiseptic agent (Garedew et al., 2004). According to the Mongolian ancient medical treatment history, the use of mumio is effective for the treatment of over 404 diseases (Frolova et al., 1998; Galgóczy et al., 2011). Many scientific and clinical research on mumio have been performed and results have shown good treatment against respiratory diseases, laryngeal papillomatosis and inflammations, bone fracture, osteomyelitis, burns and skin diseases (Stohs et al., 2017; Talbert et al., 2014). Considering the high content of mineral and proteins, this traditional medicine may support tissue regeneration and as such, has been applied in ulcer healing activity (Shahrokhi et al., 2015). Beeswax as another traditional medicine dates back to ancient Egypt (1550 B.C.), used as the main ingredient in many recipes for the preparation of ointments and creams for the treatment of burns and wounds as well as to soothe joint pain (Fratini et al., 2016; Szulc et al., 2020). A few studies showed that beeswax in synergy with other natural products possesses antimicrobic effectiveness against *staphylococcus aureus*, *salmonella enterica*, *candida albicans* and *aspergillus niger* (Carpes et al., 2007; Ghanem Nevine, 2011; Hromiš et al., 2015; Ngamekaue and Chitprasert, 2019; Voidarou et al., 2011).

During the past decade, several efforts have been made towards fabricating gelatin-based scaffolds for drug delivery and induce tissue regeneration in wound healing, either by localized or targeted approaches (Kang and Park, 2021; Yang et al., 2010; Zheng et al., 2018). Due to the ability of controlled release, different crosslinked matrices have been widely adopted as carriers for enhancing the activity of loaded bioactive drugs. Herein, we intend to enhance the performance of dual crosslinked biobased gelatin-polyvinyl alcohol interpenetrated bacterial cellulose (GT-PVA/BC) hydrogel when applied as antimicrobial wound dressings. Mumio, beeswax and cinnamon oil, representing the water-insoluble drug models were fabricated by an emulsion phase followed by integration into GT-PVA/BC hydrogel matrix to produce composite gel dressings. The effects of varying the ratio of PVA and BC on gel fraction, morphology, equilibrium swelling,

compressive modulus and degradation in vitro were examined. Finally, *in vitro* cell compatibility against lung cell (A549) lines as well as antimicrobial properties against both bacteria (*S. aureus* and *K. pneumonia*) and fungi (*C. albicans* and *A. niger*) strains were investigated in order to examine the positive effects in the prospective prevention of microbial infection during wound healing application as a dressing patch.

2. Materials and methods

2.1. Materials

Gelatin (GT) powder (Type A, from porcine skin) and polyvinyl alcohol (PVA, Mw ~67,000; 86%–89% hydrolysed) were purchased from Sigma-Aldrich. Bacterial cellulose (BC) used was biosynthesized using *Komagataeibacter xylinus* CCM 3611^T (obtained from the Czech Republic Centre for Collection of Microorganisms). Sodium tetraborate decahydrate (borax, $Na_2[B_4O_5(OH)_4]\cdot 8H_2O$ was purchased from Pentachemicals Ltd. Polyethylene glycol diglycidyl ether (PEGDE, Mn = 500 g/mol), sodium hydroxide (NaOH), methanol (MeOH, ≥99% purity) sulphuric acid (H_2SO_4, ≥95% purity) and lyophilized powder of lysozyme (from chicken egg white, protein ≥90%) were supplied by Sigma Aldrich. Cinnamon essential oil and beeswax were purchased from a commercial organic store. Mumio also known as mumijo traditional medicine was obtained from Monenzym Co., Ltd. Mongolia. Beeswax was purchased from an organic store in Zlín, Czech Republic All chemicals were used without further purification. Distilled water (dH_2O) was use for the preparation and washing samples.

2.2. Biosynthesis of bacterial cellulose

Komagataeibacter xylinus CCM 3611^T was cultivated in 10-well agar plates and incubated at 30 °C for 72 h. Each agar medium contained 100 g glucose, 10 g yeast extract, 20 g Calcium carbonate ($CaCO_3$), 25 g agar, and 1000 mL demineralized water. In brief, 5 loops of bacteria were transferred into 5 mL of liquid Hestrin and Schramm (HS) medium (containing 2.0% glucose (w/v), 0.5% yeast extract (w/v), 0.5% peptone, 0.27% Na_2HPO_4 (w/v), and 0.15% citric acid (v/v)) and incubate at 30 °C for 2 days in static culture conditions. The inoculum was then transferred to 100 mL of HS medium and kept for 15 days at 30 °C in static conditions. After 15 days, BC pellicles were harvested and cleaned by immersion in 0.5M NaOH solution at 80 °C for 1 to 2 h.

The obtained treated BC pellicles were washed with deionized water, frozen at −110 °C, freeze dried and used for further preparations.

2.3. Preparation of hydrogel

5 %w/v gelatin (GT) was prepared by dissolution in distilled water heated at 60 °C for 30 min under magnetic stirring and the pH adjusted between 8 and 9. PEDGE (2.5 %w/v) was added to the gelatin solution as the first crosslinking agent and allowed to crosslink for 2h at 60 °C. Subsequently, pre-determined amounts of PVA solution were added to the crosslinked mixture to form final concentrations of 2.5 and 4.0 %w/v. Under continuous stirring at 60 °C, BC was then added to the GT-PVA mixture in different amounts of 0.5 and 1.0 %w/v. The mixture was homogenized for 1h and the second crosslinking agent i.e., a pre-determined amount of 5 %w/v borax was added dropwise under magnetic stirring to obtain a final concentration of 0.5 %w/v. The entire mixture was quickly and continuously stirred to ensure complete homogeneity. Thereafter, the mixture was rapidly casted onto polystyrene plates and allowed to form smooth and flexible dual crosslinked gels. The samples were finally neutralized by washing several times with distilled water to remove unreacted components. The hydrogels were then subjected to freezing drying at −120 °C and the obtained dry samples designated as GP1, GP2, GPB1, GPB2, GPB3 and GPB4. Considering GP as the controls and GPB as the sample with BC. The composition of the different formulations is presented in **Table 1**.

Table 1
Composition of synthesized hydrogels.

Sample	GT (%w/v)	PVA (%w/v)	BC (%w/w)	PEDGE (%w/w)	Borax (%w/w)
GP1	5	2.5	/	2.5	0.5
GP2	5	4.0	/	2.5	0.5
GPB1	5	2.5	0.5	2.5	0.5
GPB2	5	2.5	1	2.5	0.5
GPB3	5	4.0	0.5	2.5	0.5
GPB4	5	4.0	1	2.5	0.5

2.4. Gel fraction and equilibrium fluid absorbency studies

The gel fractions of the prepared hydrogels were determined as previously reported with slight modifications (Pandey et al., 2014). Weighted amounts (*Wo*) of prepared freeze-dried samples

were immersed in dH_2O for 2 days at room temperature to remove unreacted components. The immersed samples were then removed, severally washed with dH_2O and dried to constant weight (W_F) in an oven at 60 °C. The gel fraction percentages (GF%) were subsequently estimated following the equation: $GF\% = (W_F / W_o) \times 100$.

The equilibrium swelling capacities of the hydrogels were evaluated by hydrating the lyophilized dried weighted samples in PBS (pH 7.4) at 37 °C for 48 h. The samples were removed from the swelling medium, blotted with tissue paper to remove excess water and weighed. Readings were collected in triplicates and the average value recorded. The equilibrium swelling percentages (ES%) were then calculated using the Eq. (1).

$$ES\% = \frac{S_F - S_o}{S_o} \times 100 \quad (1)$$

Where, S_o and S_F are the weights of the dry and swollen hydrogels, respectively.

2.5. Biodegradation

The degradation of prepared hydrogel patches was investigated following the enzymatic technique as previously described with slight moderations (Ngwabebhoh et al., 2021; Shamloo et al., 2021). In brief, freeze-dried disc shaped hydrogels of diameter 10 mm were initially weighed (*Wo*). In order to simulate the environment of skin tissue, the hydrogel samples were suspended in 10 mL of phosphate buffered saline (PBS, pH = 7.4) containing 0.1 mg/mL lysozyme in petri plates and were incubated at 37 °C under shaking of 100 rpm. The PBS solution was changed every 2 days and at different pre-determined time intervals, the hydrogels were washed with distilled water, dried and were weighted (*Wt*) within a period of 30 days. The residual weight percentage (*RW%*) was calculated using Eq. (2).

$$Residual\ weight\ \% = \frac{W_t}{W_o} \times 100 \quad (2)$$

2.6. Characterization techniques

Fourier transform infrared (FTIR) spectra of the hydrogel samples was analysed using a Nicolet iS5 (Thermo Scientific, USA), scanned were performed at resolution 4.0 cm^{-1} in the range of 4000

to 400 cm^{-1}. Thermogravimetric analysis was evaluated with the TA instrument Q50 V20.13 thermogravimetric analyser from 25 to 500 °C at a heating rate of 20 °C/min under a nitrogen flow rate of 60 mL/min. Surface morphology was visualized using a scanning electron microscope (SEM, FEI™, Brno, Czech) at an accelerating voltage of 5 kV. Before analysis, the samples were gold sputter-coated with a JEOL JFC 1300 Auto Fine coater for better surface conductivity. Diffraction pattern of the samples was examined using a high-resolution Mini Flex™ 600 X-ray diffractometer (Rigaku, Japan). The mechanical analysis of the hydrogels were conducted under unconfined compression at 25 °C using a Testometric MT350-5CT (Labomachine, Czech Republic). Prior to analysis, swollen hydrogels were cut into cylindrical shapes of 10 mm diameter and compressed to 80% under a static load of 5 kg and crosshead speed of 1 mm/min.

2.7. Bioactive agent loading in hydrogel

The loading process was performed by incorporating mumio (MM), beeswax (BW) and cinnamon oil (CO) into the hydrogel matrix during synthesis. The concentration of CO was kept constant at 0.1 %w/w while the concentrations of MM and BW were varied between 2 and 1 %w/w. Given the water insolubility and hydrophobicity of these bioactive components, an oil-in-water emulsion phase was first prepared to form microspheres droplets using 2-3 drops of tween 80 as the surfactant. This ensured homogenous dispersion of the bioactive components in the gel matrix. The formed emulsion phase was then transferred into the gel matrix dropwise under vigorous stirring followed by the addition of borax and the loaded hydrogel samples formed were freeze dried for further analyses. The loading capacities of the different bioactive components were determined with control samples containing single components loaded in the gel matrix. CO was determined using the supernatant extract obtained from centrifugation (Afshar et al., 2020). In brief, a pre-determined weighed CO loaded gel sample was swollen in dH_2O 8:2 MeOH, crushed and centrifuge in a 2 mL vial. The supernatant was then collected and the absorbance value of the residual CO measured using a UV-Vis single beam spectrophotometer (Model I-290) at λ_{max} = 290 nm. The loading percentage (%) was subsequently calculated using Eq. (3). On the other hand, the loading capacities of MM and BW in the hydrogel matrix was estimated by considering the weight difference between the initial weight of bioactive particulates and the final weight entrapped in the gel matrix after freeze drying (Eq. 4).

$$\text{CO loading } \% = \frac{D_L - D_S}{D_L} \times 100 \quad (3)$$

$$\text{MM or BW loading } \% = \frac{M_F}{M_i} \times 100 \quad (4)$$

Where, D_L and D_S are the concentrations of CO in the hydrogel matrix and supernatant, respectively. *Mi* is the initial weight of MM and BW incorporated in the hydrogel sample and M_F is the final dry weight of the loaded gel sample.

2.8. Cell cytocompatibility and antimicrobial assays

The cell compatibility was evaluated following MTT assay. The test samples both non-loaded (as control) and loaded GPB were sterilized by UV radiation prior to testing. Human alveolar basal epithelial (A549) cell line was seeded in RPMI1640 Medium supplemented with 10% v/v FBS and antibiotic antimycotic solution (penicillin G, 100 U/mL and spectromycin G, 100 μg/mL) in a humidified atmosphere of 95% air and 5% CO_2 at 37 ºC. In order to evaluate the cell viability effect, the cells were sub-cultivated in Trypsin- EDTA solution 0.25% for 3 min, and then the cells in seeding concentration of 1×10^5 per mL were grown in a 96-well plate for 24 h. After the adhesion phase, the medium was removed, and the cells were treated with 100 μL of the medium containing the extract of the sample (every sample/2 mL). After 24 h incubation, standard MTT assay was performed using 100 μL of RPMI1640 containing 10% MTT for 4 h and 80 μL of solubilization buffer (DMSO) for 15 min at 37 °C in CO_2 incubator. Infinite M200 Pro NanoQuant (Tecan, Switzerland) was used for measuring the absorbance at 570 nm and the reference wavelength of 690 nm.

On the other hand, the antimicrobial activity of GPB non-loaded (as control) and loaded hydrogels was tested against two bacterial (*Klebsellia pneumonia* CCM 4415 and *Staphylococcus aureus* CCM 4516) and two fungi (*Candida albicans* CCM 8215 and *Aspergillus niger* CCM 8222) strains. The inoculum suspensions were prepared using colonies after 24 h of culture. All of the utensils were sterilized at 160 °C in an oven over a period of 30 min while all the hydrogel membranes were sterilized under ultraviolet light for 30 min. All collected microbial colonies were suspended in sterile 0.9% aqueous solution of NaCl with the exception of *Aspergillus niger,* which was suspended in sterile 0.9% aqueous solution of NaCl and 0.05% polysorbate 80R. Their

densities were adjusted to the turbidity of a 0.5 Mc Farland Standard (108 colony – forming unit CFU/mL). The antimicrobial activity was then detected by the agar disc diffusion test. Accordingly, the microbial suspensions (100 μL aliquot of each stock of approximate concentration $12x10^8$ CFU/mL) were inoculated onto the surface of prepared agar plates (Tryptone soya agar TSA for bacterial test and Sabouraud Dextrose Agar SDA plates for fungal test) and sterile 9 mm diameter discs of the hydrogel samples were placed on the surface of inoculated plates. All of the samples were subsequently incubated for 24 h (bacterial) and 96 h (fungi) at 37 °C and 25 °C, respectively. The inhibition diameter zones (mean ± standard deviation) and the observed resistance of the investigated samples was then determined.

2.9. Statistical analysis

All experimental data were analyzed using Analysis of Variance (ANOVA). Statistical significance was evaluated at p-value ≤ 0.05. All results are presented as mean ± standard deviation.

3. Results and discussion

3.1. Fabrication of hydrogel

In the last decade, gelatin/PVA membranes materials have been extensively studied as wound dressing materials (Fan et al., 2016; Jaiswal et al., 2013; Shamloo et al., 2021). However, most of the membrane dressings exhibit limited applications due to their low rate of fluid absorbency, bioadhesive nature and bioactivity, which leads to slow tissue regeneration during wound healing. In this study, we postulated that the development of the mumio-based GPB integrated hydrogel dressing with high bioactivity and considerable mechanical performance would greatly contribute to the application of wound healing. This antimicrobial hydrogel dressing patch was synthesized by mixing the crosslinked solution of gelatin with PVA followed by semi-interpenetration with BC (**Fig. *1***a). The first crosslinked network was formed via PEDGE mediated crosslinking by epoxy ring opening with the free amino groups ($-NH_2$) of gelatin. This was followed by the green crosslinking mechanism obtained via the formation of interchain diol–borate complexes that led to the crosslinking of PVA within the gelatin and BC network. To enhance antimicrobial properties of the hydrogel patches, mumio, beeswax and cinnamon oil loaded GPBs were fabricated by

emulsion dispersion in the hydrogel matrix to produce composite dressings (**Fig. *1***b). The loading capacity of mumio, beeswax and cinnamon oil was determined as 88.9 ± 1.92%, 92.3 ± 1.32%, and 74.3 ± 0.92%, respectively.

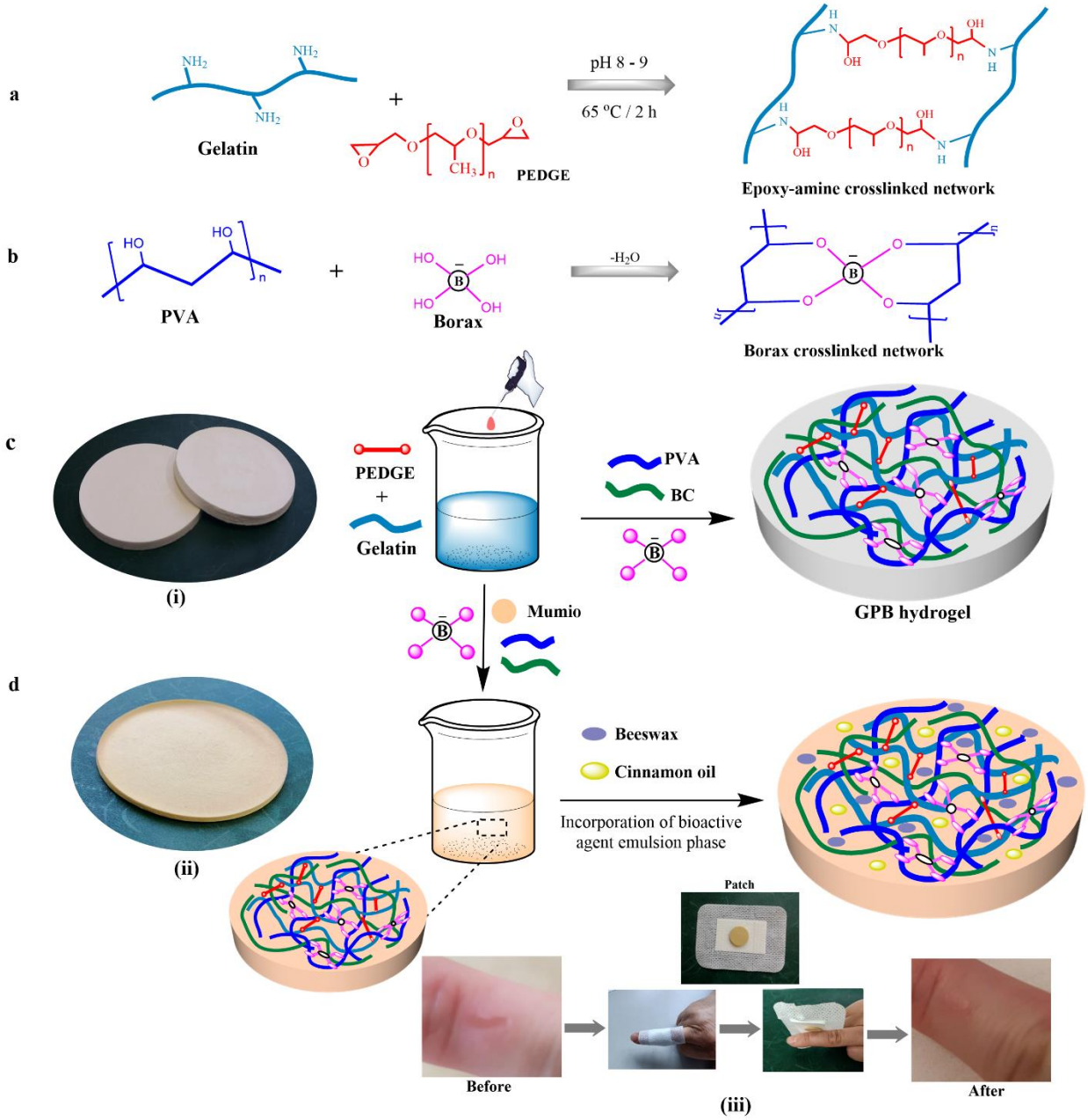

Fig. 1. Schematic representation of (a) Gelatin-PEDGE and (b) PVA-borax crosslinking reactions. (c) Gelatin-PVA/bacterial cellulose wound dressing hydrogel after freeze drying and the illustration of the blend formation and crosslinking network formed. (d) Depicting the preparation of the mumio-based wound dressing gel material and the loading of the different bioactive agents of beeswax and cinnamon oil in the hydrogel matrix. Insert images show the obtained freeze-dried (i) non-loaded and (ii) loaded hydrogel samples. (iii) Shows a prepared patch sample use in the treatment of a swollen scar on the finger depicting the before and after appearance.

3.2. Characterization of hydrogel patch

3.2.1. FTIR analysis

Infrared absorbance spectra of gelatin, PVA, BC, GP and GBP hydrogels are illustrated in **Fig. 2**a. The IR spectra of gelatin shows amide I, II and III bands at 1645, 1537 and 1244 cm^{-1}, respectively. The amide I band attributes to C=O stretching while amide II and amide III bands represent NH bending. Another characteristic band can be observed at 3301 cm^{-1} which ascribes to the NH-stretching and hydrogen bonding (El Fawal et al., 2021). PVA IR spectra shows broad absorption band at 3347 cm^{-1} which is due to the O-H stretching of PVA hydroxyl groups. An intense absorption band at 1722 cm^{-1} can be seen which identifies to acetate group carbonyl (C=O) stretching. C-H stretching vibrations of backbone aliphatics can be linked to 2940 and 2910 cm^{-1}. Strong absorption peaks at 1082 and 1251cm^{-1} correspond to C-O stretching and CH-OH combination frequencies, respectively (Patwa et al., 2020a). BC nanofibers showed characteristic peaks at 3347, 2923, 1745 and 1051 cm^{-1}, which attribute to the –CH group stretching vibration, -OH group bending vibration, -C-O-C- pyranose ring and –CH deformation of cellulose I structure in BC, respectively (Ngwabebhoh et al., 2021). The carbonyl peaks of gelatin and PVA combine and give rise to a broader peak at 1660 cm^{-1} and a shoulder at 1691 cm^{-1} which indicates good compatibility between gelatin and PVA in GP hydrogels. With incorporation of BC, the intensity of the hydrogen bonding starting from 3000 to 3624 cm^{-1} band is higher as compared to individual components. The plausible reason for this could be hydrogen bond formations between PVA, gelatin and bacterial cellulose resulting in more stable GPB hydrogels.

3.2.2. X-ray diffraction analysis

Fig. 2b displays the X-ray diffraction patterns of Gelatin, PVA, BC, GP and GPB hydrogels. Gelatin displays its characteristic triple-helical crystalline structure with two broad peaks at 9.60° and 22.5°. PVA shows peak positions at 20.5° and a shoulder at 23.5° which matches with the literature (Patwa et al., 2020a). The BC pellicle showed sharp peaks at 14.3°, 16.7° and 22.2° which points towards higher crystallinity as compared to gelatin (Ngwabebhoh et al., 2021). GP hydrogels showed a broad peak at $2\theta = 19.1°$ because of combination of gelatin and PVA reflections. However, for GPB hydrogels the peak intensity improved upon incorporation of BC which indicated increase in crystallinity. The presence of BC in GPB can be confirmed by the peak

reflection at 22.3°, this slight shift in peak position may be due to possible layering of BC in between polymer matrix.

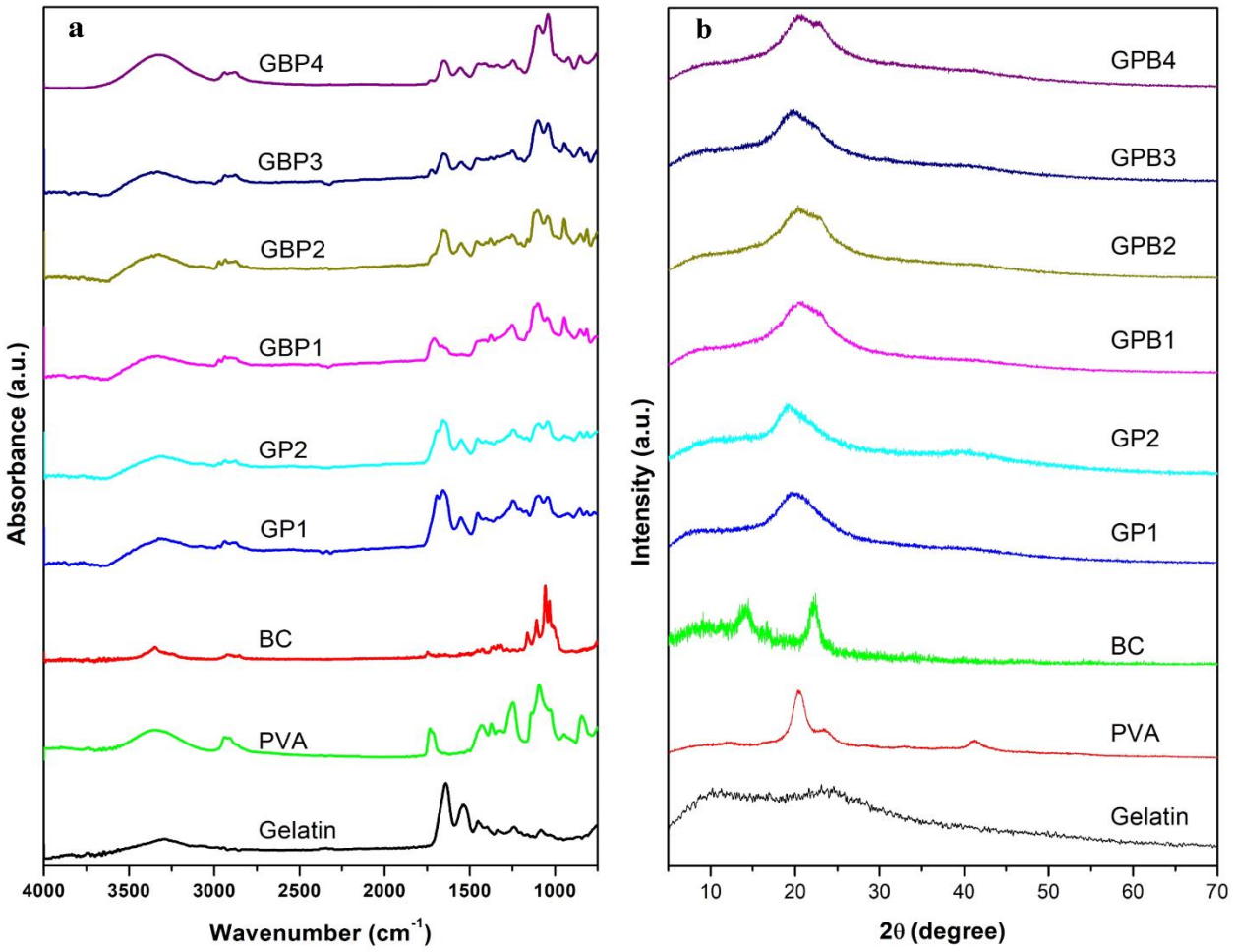

Fig. 2. (a) Attenuated total reflectance (ATR) mode FTIR spectra and (b) X-ray diffractograms of gelatin, PVA, BC, freeze-dried GP and GPB hydrogels.

3.2.3. Surface morphology of prepared hydrogels

Morphological Analysis of GP and GPB Hydrogels The cross-sectional morphologies of the lyophilized GP and GPB hydrogels were investigated and their representative SEM micrographs are shown in **Fig. 3**. The micrographs were recorded at 250× and 1000× to study the pore structure, compatibility of gelatin and PVA and distribution of BC network inside the hydrogels. GP1 hydrogels showed an overall smooth appearance with micron-sized pores which indicates good compatibility between gelatin and PVA. With increase in PVA concentration in GP2, the pore structure becomes denser. With incorporation of BC, the pore structure changes drastically and the

surface becomes rough with further decrease in pore size. Similar observations were made in previous studies when BC was used as reinforcement (Ngwabebhoh et al., 2021; Patwa et al., 2020b). With 1wt.% BC loading the pore structure becomes homogeneous with absence of larger pores as seen when 0.5wt.% BC was added.

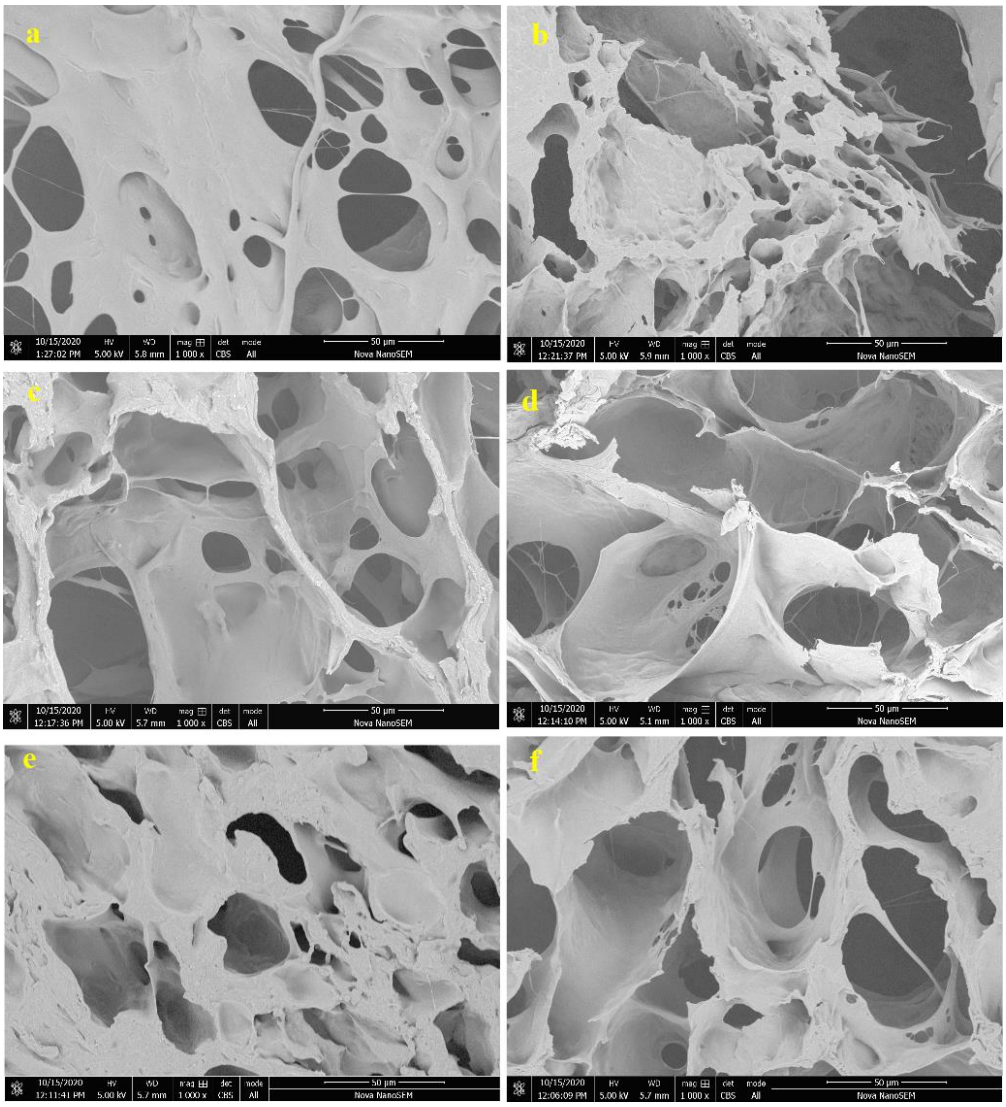

Fig. 3. FE-SEM micrographs at 1000x for prepared (a) GP 1, (b) GP 2, (c) GPB 1, (d) GPB 2, (e) GPB 3 and (f) GPB 4 hydrogels.

Gel fraction, swelling and in vitro degradation

The gel fraction values of the prepared different hydrogels are presented in **Fig. 4**a. According to the deduced results, the highest gel fractions were observed for gels containing BC, which was expected since BC increased interfacial interaction via hydrogen bonding with the crosslinked

gelatin-PVA system. The gel fractions for the prepared hydrogels were determined as 88.21 ± 2.56%, 90.13 ± 2.42%, 90.89 ± 2.49%, 91.98 ± 2.31%, 93.23 ± 2.05%, and 95.20 ± 2.61% for GP1, GP2, GPB1, GPB2, GPB3, and GPB4, respectively. Considering the gel fraction depicts the crosslinking density in the gel structure, the data indicates that the addition of BC for the various PVA concentrations increased the gel fraction since it encouraged more chain entanglement and restrictions on the crosslinked gelatin and PVA chains. This creates more physical crosslinks, adding to those present via crosslinking of gelatin and PVA systems.

The equilibrium swelling ratio is one of the most important parameters used to evaluate hydrogels. **Fig. 4**b shows the swelling dynamics of the prepared GP and GPB hydrogels. It can be found that the swelling capabilities of the hydrogels with BC particularly that with higher PVA and BC concentrations (GPB4) was highest compared to samples without BC, indicating that the addition of BC significantly improved the swelling property of the hydrogels. This is attributed to the interaction with gelatin and PVA as well as the physical networks formed in the hydrogel systems, which could slowly expand to contain more water (Spoljaric et al., 2014). The effect of variation in PVA concentration can also be observed. By increasing the concentration of PVA from 2.5%wt (GPB and GPB2) to 4%wt (GPB3 and GPB4) at constant gelatin and BC concentration greatly increased the swelling capacities of the gels from 244 ± 10.74% to 289 ± 12.87% for GPB1 and GPB3 as well as from 345 ± 17.29% to 396 ± 19.82% for GPB2 and GPB4, respectively. It is well known that swelling decreases with the increase in crosslinking density. Thus, at constant crosslink density for both PEDGE and borax while increasing the concentration of PVA and BC, the swelling capacity of the hydrogels will increase owing to the availability of a greater number of vacant hydroxyl groups on polymer molecules. This enhances hydrogen bonding with the water molecules and thus increases the uptake of water in the hydrogel structure. In addition, the increase in free volume and chain mobility are characteristic of physically crosslinked hydrogels. Therefore, at high concentration of PVA and BC at constant low crosslinker amount, structural restraints are low creating the ability of water molecules to penetrate, adhere and ultimately swell the hydrogel (Bai et al., 2018). Chang et al. reported a similar behavior based on prepared PVA–cellulose hydrogels, where they observed an increase in swelling ability with PVA and nano-fibrillated cellulose concentration (Chang et al., 2008). The obtained results suggested that there was sufficient physical interaction between cellulose and PVA, which enhanced water adhesion and uptake while maintaining a stable hydrogel structure.

The degradation profiles of the prepared hydrogels, with various amounts of PVA and BC immersed in lysozyme solution is shown in **Fig. 4**c. The degradation of the hydrogels is a time-dependent process. Based on results obtained, the hydrogels without BC (GP1 and GP2) degraded faster when compared to the samples BC (GPB1, GPB2, GPB3, GPB4). The fast degradation in GP hydrogels is mainly attributed to the high ratio of gelatin to the total polymer composition in the gel structure rendering it more to be more soluble in water. As the gels start to dissolve, the formed voids within the structure facilitate the disintegration rate of the hydrogels. By incorporating BC in the hydrogel matrix, significantly decreases the rate of degradation of the hydrogel dressings. Interestingly, all the hydrogels lost more than 50% of their weights after 15 days of degradation except for GPB4 with high PVA and BC concentrations (4%wt and 1%wt, respectively) that showed low degradation. These results support the speculation that BC acts as a filler/reinforcer. As such, enhances interfacial hydrogen bond interaction between PVA and BC thereby increasing crosslinking density in the gel structure, leading to increase in degradation resistance (Hussein et al., 2021).

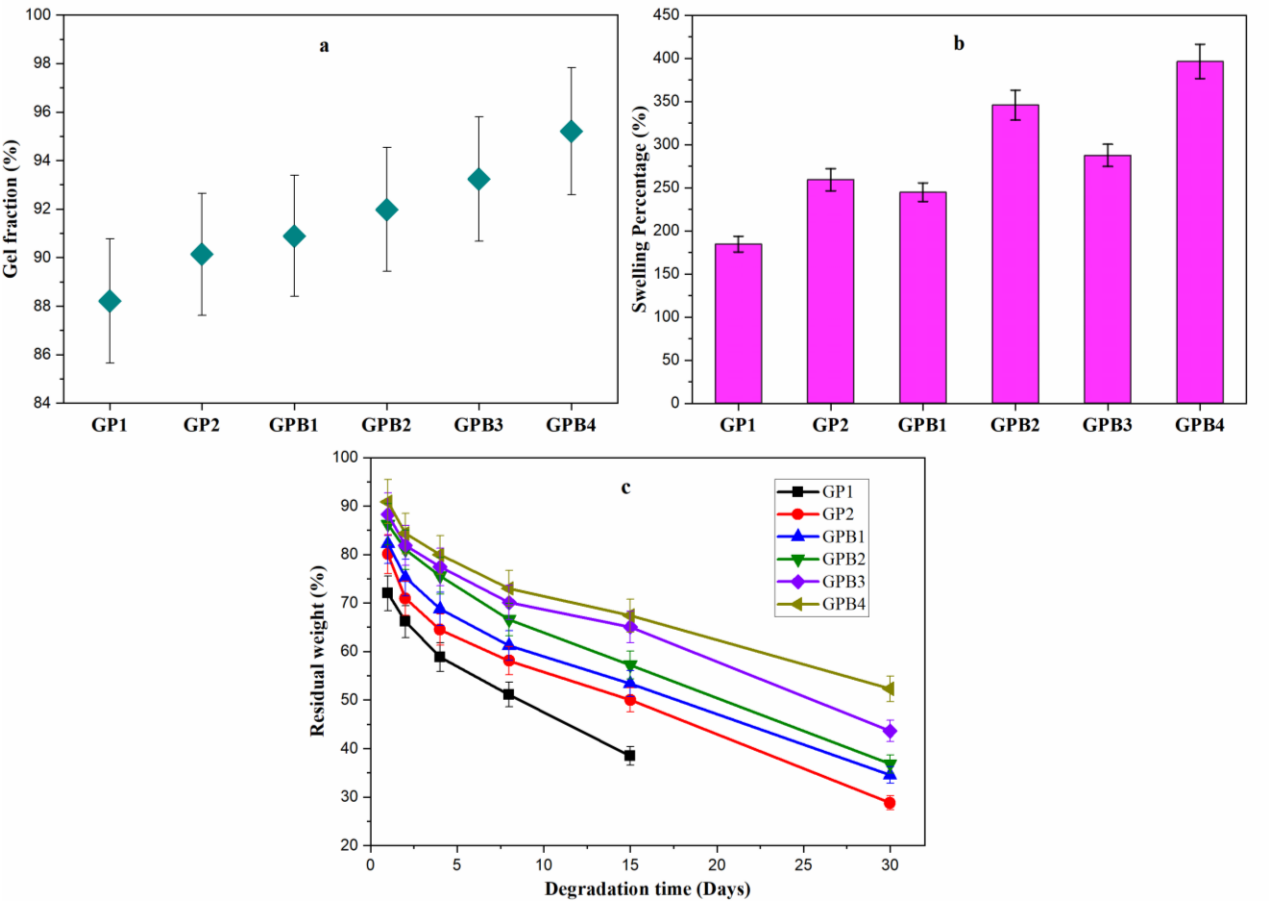

Fig. 4. (a) Gel fraction of prepared hydrogels. (b) *In vitro* equilibrium swelling and (c) degradation of the different gels as a function of time in PBS at 37 °C. Values reported are an average of n = 3, ±standard deviation.

3.2.4. Compression analysis

The compressive properties of the prepared GP and GPB hydrogels were investigated at 25 °C (**Fig. 5**). The stress–strain curves of hydrogels obtained via static compression mode are depicted in **Fig. 5**a and compressive modulus obtained as shown in **Fig. 5**b. As observed, the compressive strength increased with the increase in the concentration of PVA from 2.5 to 4 %w/v (GP1 and GP2). However, the addition of 0.5 %w/v BC greatly impacted the compressive modulus, increasing from 3.06 ± 0.29 kPa for GP1 to 17.81 ± 1.32 kPa for GPB1 and 7.29 ± 1.26 kPa for GP2 to 29.55 ± 1.49 kPa for GPB3. In addition, an increase in the concentration of BC from 0.5 to 1 %w/v increased the compressive modulus of the gels from 17.81 ± 1.32 kPa for GPB1 (2.5%PVA / 1%BC) to 26.72 ± 0.58 kPa for GPB2 (2.5%PVA / 0.5%BC) and 29.55 ± 1.49 kPa for GPB3 (4%PVA / 0.5%BC) to 37.41 ± 1.68 kPa for GPB4 (4%PVA / 1%BC). Similar behavior was exhibited by the maximum stress, with the highest values obtained at PVA and BC loadings of 4%wt and 1wt%, respectively. The obtained moduli values are significantly higher than those reported by Han et al. (Han et al., 2013), which they prepared PVA–borax incorporated nanocellulose hydrogels with moduli values determined in the range from 3.8 to 22.5 kPa. The increase in mechanical properties is attributed to the reinforcing impact of cellulose nanofibrils. Also, the semi-interpenetrating network formed by BC, enhanced interfacial interactions between gelatin, PVA and BC thereby impart restricting the segments of polymer chain during deformation leading to enhanced strength and stability (Spoljaric et al., 2014). Entangled segments of BC fibrils act as physical crosslinks, working in conjunction with PEDGE and borax crosslinks towards generating mechanical integrity of the hydrogels. This is supported by the increased gel content observed at PVA and BC concentrations up to and including 4wt% and 1%wt, respectively. At increased of PVA and BC loadings, the gels were non-homogenous, thereby affecting the final compressive strength. A probable cause for this is very high concentrations of BC prevents effective crosslinking between PVA and borax. Although the crosslinking of gelatin as well as the hydrogen bonds between the various polymers contribute to the mechanical behavior of the hydrogels, the crosslink complexation between PVA and borax is very crucial. Based on pre-experimental evaluations, an increase in borax concentration at constant gelatin, PVA and BC

amounts of 5wt%, 4%wt and 1%wt, respectively, led to non-homogenous gels being formed. As such, the concentration of borax was maintained ideally at 0.5%wt. Moreover, higher borax loadings depict reduced free volume thereby forming confined structure leading to reduced polymer chain mobility resulting in stiffer and stronger gels (Han et al., 2014).

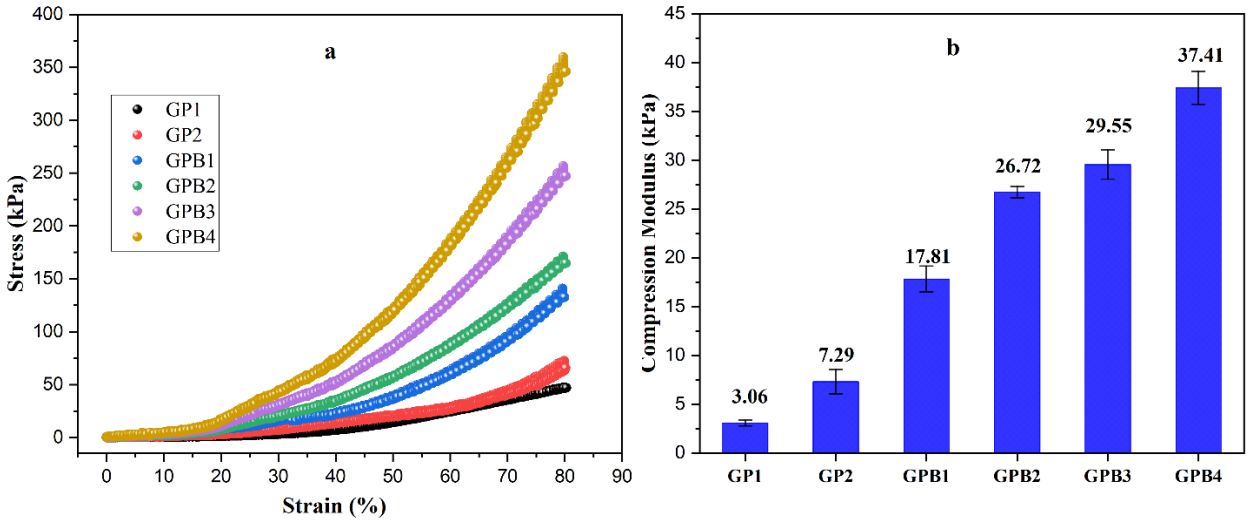

Fig. 5. (a) Stress-strain curve of the different prepared hydrogels at 25 °C. (b) Compressive moduli of hydrogels calculated from the stress-strain curves. Values reported are an average n = 3, ± standard deviation.

3.2.5. Thermogravimetric analysis

Thermal stability is a desirable property in hydrogel processing. The thermal degradation profiles of GP and GPB hydrogels were recorded from 25 to 500 °C under inert gas environment and are illustrated in **Fig. 6**a. It can be seen that the thermal profiles of both materials are quite similar to each other. However, upon close inspection of the derivative thermogravimetric profiles shown in **Fig. 6**b, it can be clearly observed that upon incorporation of BC, the degradation peaks shifted from 331 °C to a higher degradation temperature of 337 °C. Hence, it is evident that addition of BC improved thermal stability of gelatin-polyvinyl alcohol hydrogels. Similar results were reported by Patwa et. al. (Patwa et al., 2020b). Both samples showed broad peak from 40 to 110 °C, which denotes the removal of bound water from the hydrogels.

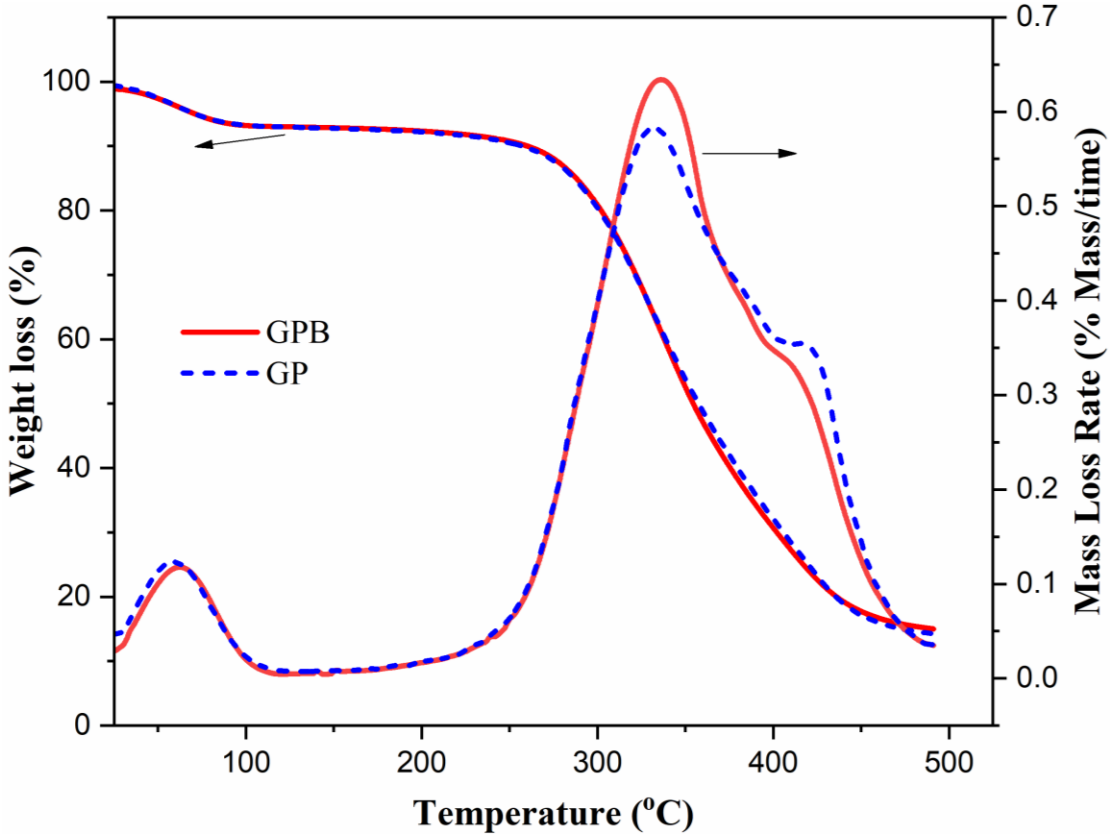

Fig. 6. Thermogravimetric (TG) and derivative TG thermal profiles for GP and GPB hydrogels.

3.3. Analysis of mumio-impregnated gels

The FTIR spectra of the pristine bioactive components of MM, BW and CO as well as loaded hydrogels with varying loading concentrations are presented in **Fig. 7**. Several distinct peaks characteristic of MM, BW and CO are observable. MM sample was characterized by relatively few broad peaks. The spectrum displayed a broad band between 3250 to 3550 cm^{-1} due to the vibration of hydrogen bonded -OH of the phenolic functional group. The peaks at 1605 and 1410 cm^{-1} may be ascribed to the aromatic C─C double bond and -OH bending vibrations of COOH group, respectively. The peak at 1050 cm^{-1} may be related to Si-OR vibration (Rehan et al., 2017). For BW, the absorption bands are characterized by hydrocarbons asymmetric stretching vibrations of CH_3 groups at 2920 cm^{-1}, asymmetric and symmetric stretching vibrations of CH_2 groups at 2860 cm^{-1}, and scissor deformation vibrations of CH_2 groups at 1460 cm^{-1} (Špaldoňová et al., 2020). In addition, the C═O stretching vibrations at 1736 cm^{-1} and C─H bending vibrations at 1180 cm^{-1} are ascribed to the ester and free fatty acids which are valuable and characteristic absorption bands for the detection of monoesters in beeswax (Tanner and Lichtenberg-Kraag,

2019). The spectral characteristic fingerprint peaks for CO are mostly between 1800 - 600 cm^{-1}. The typical peaks at 1670 and 1630 cm^{-1} are associated to the stretching vibration of the aldehyde carbonyl (C═O). These distinct peaks relates to high levels of cinnamaldehyde and aldehydes in the volatile oil of cinnamon (Li et al., 2013). The peak at 1120 cm^{-1} is attributed to the stretching and deformation vibrations of C─O and the C─OH. The peak at 973 cm^{-1} is ascribed to C─H bending vibration. As for the IR spectra of the loaded hydrogel samples with the different bioactive components, shows a total overlap of the main absorption peaks for the various components with that of GPB hydrogel. The several characteristic peaks observed for GPB hydrogel (see description in **Fig. 2**a) are evident in the loaded samples. However, comparing the peak intensity of the non-loaded and loaded gel samples reveals sharper and larger peaks at 2880 – 2950 cm^{-1} and 1730 cm^{-1}, which are presumably more prominent within the loaded hydrogels than non-loaded. Confirming interaction of the bioactive compounds with hydrogel the system.

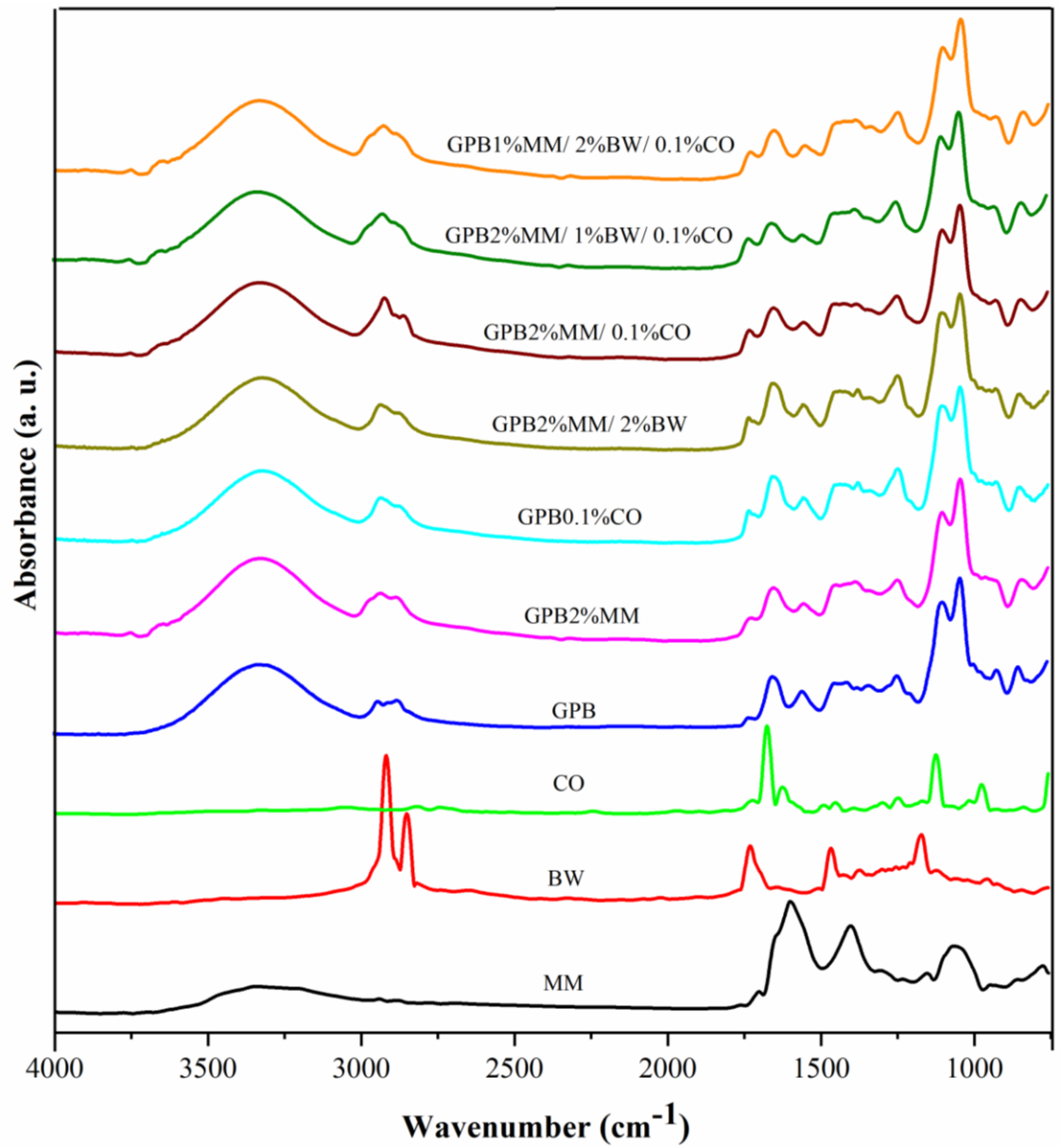

Fig. 7. FTIR spectra of loaded GPB hydrogel with mumio (MM), beeswax (BW) and cinnamon oil (CO) as bioactive drugs.

Scanning electron (SEM) images highlighting the influence of the bioactive components' concentration on GPB hydrogel morphology are presented in **Fig. 8**. The three-dimensional porous network morphology is evident due to water removal. The voids/pores formed following the removal of water are approximately spherical in shape and exhibit a diameter of ~200 µm. BC fibril aggregates are observable protruding through the network, indicating its interaction with gelatin and poly(vinyl) alcohol (Treesuppharat et al., 2017). All samples show similar morphology, with negligible differences in void shape and size visible. This confirms that the bioactive

components of mumio, beeswax and cinnamon oil homogenously interacted with the crosslinked polymer gel matrix. Furthermore, the hydrogels' structure is slightly influence by solution viscosity after incorporation of the bioactive components when compared to the non-loaded GPB hydrogel (see Fig. 4). Addition of the bioactive components resulted in denser and compact materials particularly for samples containing mumio since it is non-soluble and disperse in the hydrogel matrix as particulates/filler. Similar observations have been reported by Chen et al. in the preparation of PVA/nanoclay gels (Chen et al., 2014).

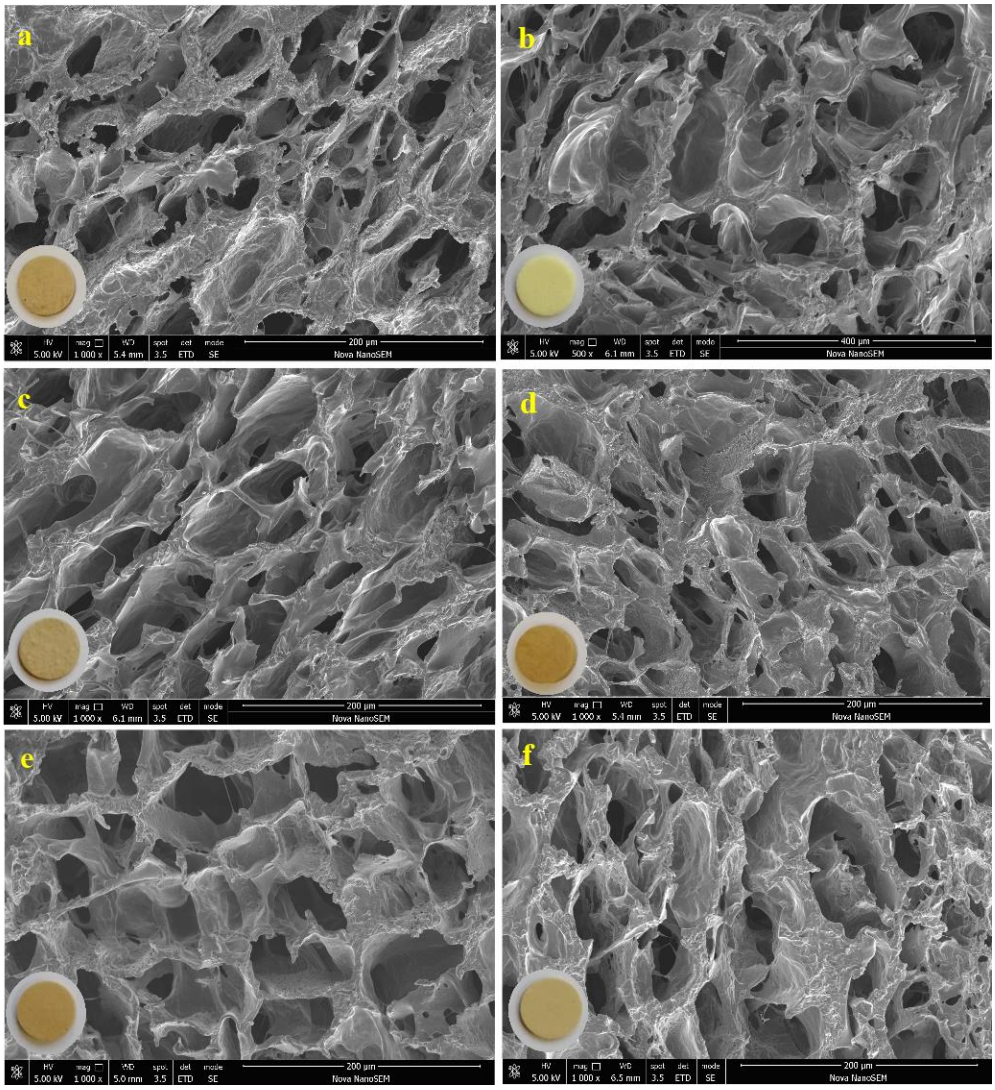

Fig. 8. SEM photographs at 1000x of loaded GPB hydrogel after lyophilization containing different ratios of bioactive drugs (MM = mumio, BW = beeswax and CO = cinnamon oil). (a) 2%MM, (b) 0.1%CO, (c) 2%MM/2%BW, (d) 2%MM/0.1%CO, (e) 2%MM/1%BW/0.1%CO and (f) 1%MM/2%BW/0.1%CO.

3.4. Cell cytotoxicity assay of loaded gels

To evaluate cell cytotoxicity of GPB loaded hydrogel dressings, *in vitro* human alveolar basal epithelial (A549) cell culture was performed, using the gels without bioactive components as comparison. Measured by MTT assay, cell viability in the different prepared loaded hydrogel dressings was lower ($p < 0.05$) than that of the control (**Fig. 9**). However, the cell viability levels of GPB2%MM and GPB2%MM/1%BW/0.1%CO (85.90 ± 4.29% and 78.24 ± 3.91%, respectively) were above 70%, indicating the samples were relative non-toxic and their incorporation as antimicrobial bioactive components can promote cell proliferation, in particular at the longer culture period. On the other hand, the very low cell viability for was observed for GPB0.1%CO and GPB2%MM/0.1%CO. Considering CO is an essential oil, this low cell viability may be attributed to the general cytotoxic effects depicted by essential oils (Dorri et al., 2018; Dušan et al., 2006). But by incorporating the other bioactive components significantly improves cell viability and thus provides a support to the hypothesis that using CO in combination with mumio and beeswax depicts a good drug system with no significant toxicity.

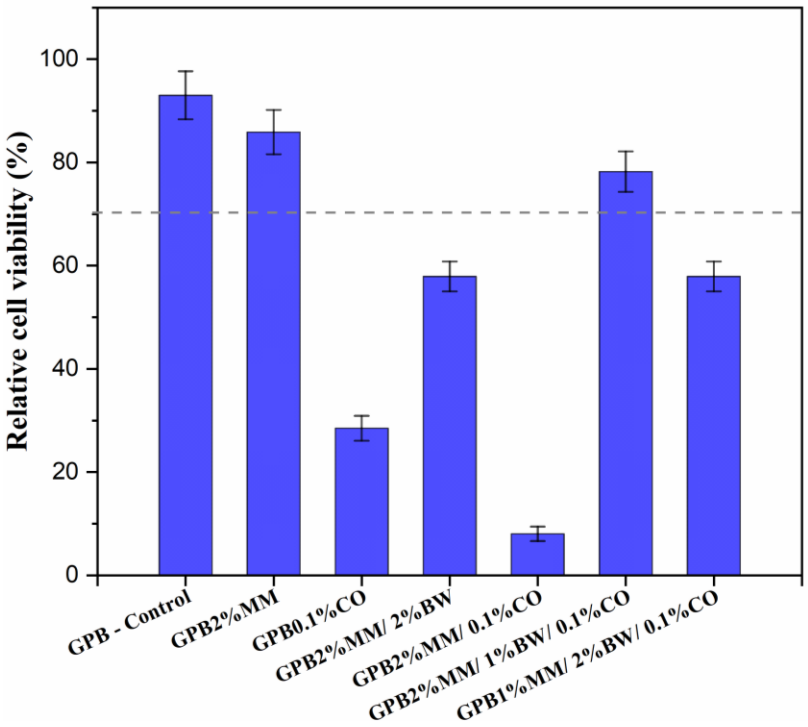

Fig. 9. Viability of human alveolar basal epithelial cells *in vitro* cultured for the different loaded GPB gel samples after 24 h at 37 ºC. Cell seeding density was 1×10^5 cells/well. Values reported are an average n = 3, ± standard deviation.

3.5. Antimicrobial activity of loaded gel dressings

The antimicrobial activity of loaded mumio-based hydrogel dressings was tested in the presence of *Staphylococcus auras* and *Klebsiella pneumoniae* as bacteria as well as for *Candida albicans* and *Aspergillus niger* as fungi. The hydrogels were placed into petri dishes containing the culture medium and then incubated at 37 °C for 24 h (bacteria) and 25°C for 96 h (fungi) to determine the resistance and growth inhibition of microbes. The results obtained from the antimicrobial assay are shown in **Fig. 10**. As observed, all investigated loaded samples were resistant against evaluated microorganisms. Comparing the control samples without bioactive components with no sign of inhibition, all loaded samples should some level of growth inhibition. The growth inhibition effects of GPB loaded against the various investigated microorganisms are exhibited in **Table 2**. According to the results, the highest growth inhibition was against *Aspergillus niger*. Nevertheless, one can conclude that GPB loaded gels possesses good antimicrobial since the growth of the microbes particularly fungi were significantly inhibited, a pretty good effect in the aspect of inhibiting the growth of microorganisms ($p < 0.05$).

Table 2
Antimicrobial activity of GPB loaded hydrogel dressings against bacteria and fungi microbes expressed in terms of diameter of inhibition zone.

Samples	Diameter of inhibition zones (mm)			
	Bacteria		Fungi	
	S.aures (+)	*K. pneumoniae (-)*	*C. albicans*	*A. niger*
GPB2%MM	1.10 ± 0.12	1.20 ± 0.15	1.12± 0.26	10.10 ± 0.38
GPB0.1%CO	1.60 ± 0.26	1.30 ± 0.19	1.2± 0.11	4.25 ± 0.19
GPB2%MM/ 2%BW	1.21 ± 0.30	1.02 ± 0.23	5.10 ± 0.11	6.28 ± 0.21
GPB2%MM/ 0.1CO	1.13 ± 0.19	1.11± 0.16	4.75 ± 0.18	15.70 ± 0.25
GPB2%MM/ 1%BW/ 0.1%CO	1.23 ± 0.21	1.30 ± 0.21	4.80 ± 0.49	15.38 ± 0.12
GPB1%MM/ 2%BW/ 0.1%CO	1.21 ± 0.17	1.00 ± 0.11	2.30 ± 0.27	8.50 ± 0.50

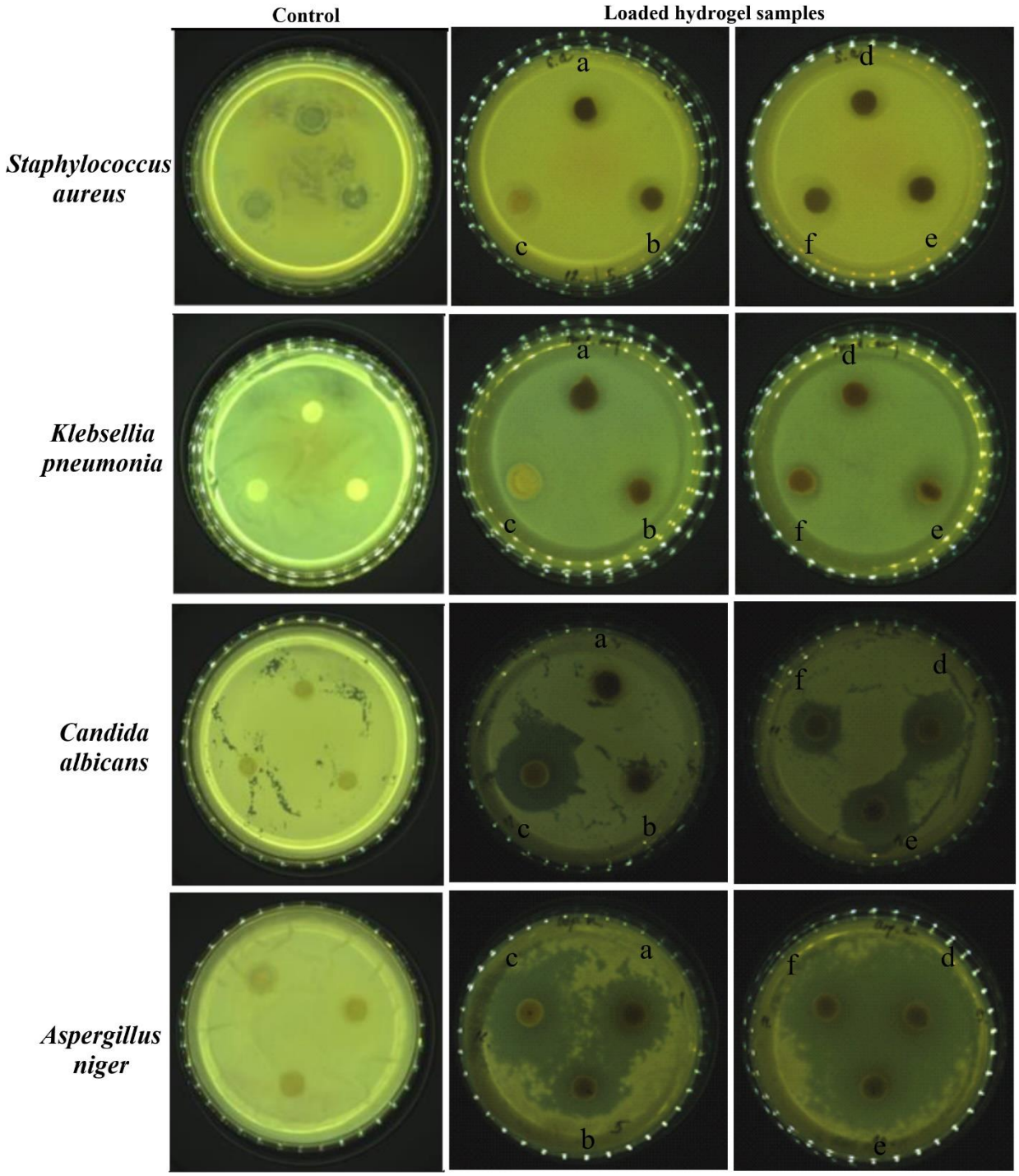

Fig. 10. Photographic images inhibition zones of loaded GPB hydrogels after incubation at 37 °C (*S. aureus* and *K. pneumonia*) and 25 °C (*C. albicans* and *A. niger*) for 24 h and 96 h, respectively. Where the loaded hydrogels are annotated as a = 2%MM, b = 2%MM/2%BW, c = 0.1%CO, d = 2%MM/0.1%CO, e = 2%MM/1%BW/0.1CO and f = 1%MM/2%BW/0.1%CO.

4. Conclusions

In summary, novel GT-PVA/BC hydrogel embed with MM containing BW and CO was dual crosslinked as wound dressing patch. Different amount of PVA and BC were added into the matrix and showed significant effect on the properties of the hydrogel. With the appropriate increase of PVA and BC, the swelling capacity, *in vitro* degradation and mechanical stability of the hydrogel was significantly improved. According to morphological analysis, the incorporation particularly of MM in the matrix was homogenous and the hydrogel showed a microporous structure. The antimicrobial test demonstrated strong resistance and inhibition effects against both bacteria (*S. aureus* and *K. pneumonia*) and fungi (*C. albicans* and *A. niger*) strains investigated. The hydrogel patches with cinnamon oil exhibited an outstanding antimicrobial activity against the investigated microorganisms but high cell toxicity for gel samples containing 0.1%CO and 2%MM/0.1%CO. In summary, the composite dressings depicted excellent resistance and growth inhibition effects against microbial infection. Thus, it can be anticipated that the antimicrobial composite materials with sufficient minimal CO concentration may provide high therapeutic efficiency as dressings patches to improve wound healing.

Author contributions

This study conceptualization and methodology was performed by Oyunchimeg Zandraa and Fahanwi Asabuwa Ngwabebhoh. Formal analysis was done by Oyunchimeg Zandraa, Rahul Patwa, Hau Trung Nguyen and Marjan Motiei. Investigation and data curation were carried out by Oyunchimeg Zandraa. Writing-original draft preparation was done by Oyunchimeg Zandraa, Fahanwi Asabuwa Ngwabebhoh and Rahul Patwa. The paper was reviewed and edited by Nabanita Saha and Petr Saha. Funding acquisition was done by Tomas Saha and Petr Saha.

Declaration of competing interest

The authors declare no competing financial interest.

Acknowledgements

The authors acknowledge the support of this work by Tomas Bata University in Zlin and the Ministry of Education, Youth & Sports of the Czech Republic - DKRVO (RP/CPS/2020/005). In

addition, great thanks to the Internal grant (projects: IGA/CPS/2020/005) from Tomas Bata University in Zlin, Czech Republic.

References

Afshar, M., Dini, G., Vaezifar, S., Mehdikhani, M., Movahedi, B., 2020. Preparation and characterization of sodium alginate/polyvinyl alcohol hydrogel containing drug-loaded chitosan nanoparticles as a drug delivery system. Journal of Drug Delivery Science and Technology 56, 101530.

Aiello, A., Fattorusso, E., Menna, M., Vitalone, R., Schröder, H.C., Müller, W.E., 2011. Mumijo traditional medicine: fossil deposits from antarctica (chemical composition and beneficial bioactivity). Evidence-Based Complementary Alternative Medicine 2011.

Albu, M., Ferdes, M., Kaya, D., Ghica, M., Titorencu, I., Popa, L., Albu, L., 2012. Collagen wound dressings with anti-inflammatory activity. Molecular Crystals and Liquid Crystals 555, 271-279.

Bai, H., Li, Z., Zhang, S., Wang, W., Dong, W., 2018. Interpenetrating polymer networks in polyvinyl alcohol/cellulose nanocrystals hydrogels to develop absorbent materials. Carbohydrate Polymers 200, 468-476.

Cacicedo, M.L., Castro, M.C., Servetas, I., Bosnea, L., Boura, K., Tsafrakidou, P., Dima, A., Terpou, A., Koutinas, A., Castro, G.R., 2016. Progress in bacterial cellulose matrices for biotechnological applications. Bioresource Technology 213, 172-180.

Carpes, S.T., Begnini, R., Alencar, S.M.d., Masson, M.L.J.C.e.A., 2007. Study of preparations of bee pollen extracts, antioxidant and antibacterial activity. Ciência e agrotecnologia 31, 1818-1825.

Chang, C., Lue, A., Zhang, L., 2008. Effects of crosslinking methods on structure and properties of cellulose/PVA hydrogels. Macromolecular Chemistry Physics 209, 1266-1273.

Chen, H.-B., Hollinger, E., Wang, Y.-Z., Schiraldi, D.A., 2014. Facile fabrication of poly (vinyl alcohol) gels and derivative aerogels. Polymer 55, 380-384.

Chen, H., Xing, X., Tan, H., Jia, Y., Zhou, T., Chen, Y., Ling, Z., Hu, X., 2017. Covalently antibacterial alginate-chitosan hydrogel dressing integrated gelatin microspheres containing tetracycline hydrochloride for wound healing. Materials Science and Engineering: C 70, 287-295.

Chiaoprakobkij, N., Suwanmajo, T., Sanchavanakit, N., Phisalaphong, M., 2020. Curcumin-Loaded Bacterial Cellulose/Alginate/Gelatin as A Multifunctional Biopolymer Composite Film. Molecules 25, 3800.

Cielecka, I., Szustak, M., Gendaszewska-Darmach, E., Kalinowska, H., Ryngajllo, M., Maniukiewicz, W., Bielecki, S., 2018. Novel Bionanocellulose/kappa-Carrageenan Composites for Tissue Engineering. Appl. Sci.-Basel 8, 22.

Das, S., Subuddhi, U., 2019. Controlled delivery of ibuprofen from poly(vinyl alcohol)−poly(ethylene glycol) interpenetrating polymeric network hydrogels. Journal of Pharmaceutical Analysis 9, 108-116.

de Oliveira Barud, H.G., da Silva, R.R., da Silva Barud, H., Tercjak, A., Gutierrez, J., Lustri, W.R., de Oliveira, O.B., Ribeiro, S.J.L., 2016. A multipurpose natural and renewable polymer in medical applications: Bacterial cellulose. Carbohydrate Polymers 153, 406-420.

Deshpande, D.S., Bajpai, R., Bajpai, A., 2012. Synthesis and characterization of polyvinyl alcohol based semi interpenetrating polymeric networks. J. Polym. Res. 19, 9938.
Dorri, M., Hashemitabar, S., Hosseinzadeh, H., 2018. Cinnamon (Cinnamomum zeylanicum) as an antidote or a protective agent against natural or chemical toxicities: a review. Drug Chemical Toxicology 41, 338-351.
Dumanli, A.G., 2017. Nanocellulose and its Composites for Biomedical Applications. Curr. Med. Chem. 24, 512-528.
Dušan, F., Marián, S., Katarína, D., Dobroslava, B., 2006. Essential oils—their antimicrobial activity against Escherichia coli and effect on intestinal cell viability. Toxicology in Vitro 20, 1435-1445.
El Fawal, G., Hong, H., Mo, X., Wang, H., 2021. Fabrication of scaffold based on gelatin and polycaprolactone (PCL) for wound dressing application. Journal of Drug Delivery Science and Technology, 102501.
Erdagi, S.I., Ngwabebhoh, F.A., Yildiz, U., 2020. Genipin crosslinked gelatin-diosgenin-nanocellulose hydrogels for potential wound dressing and healing applications. International Journal of Biological Macromolecules 149, 651-663.
Fan, L., Yang, H., Yang, J., Peng, M., Hu, J., 2016. Preparation and characterization of chitosan/gelatin/PVA hydrogel for wound dressings. Carbohydrate polymers 146, 427-434.
Fratini, F., Cilia, G., Turchi, B., Felicioli, A., 2016. Beeswax: A minireview of its antimicrobial activity and its application in medicine. Asian Pacific Journal of Tropical Medicine 9, 839-843.
Frolova, L., Kiseleva, T., Kolkhir, V., Baginskaya, A., Trumpe, T., 1998. Antitoxic properties of standard dry mumijo extract. Pharmaceutical Chemistry Journal 32, 197-199.
Galgóczy, L.N., Guba, M., Papp, T., Krisch, J., Vágvölgyi, C., Tserennadmid, R., 2011. In vitro antibacterial effect of a mumijo preparation from Mongolia. African Journal of Microbiology Research 5, 3832-3835.
Garedew, A., Feist, M., Schmolz, E., Lamprecht, I., 2004. Thermal analysis of mumiyo, the legendary folk remedy from the Himalaya region. Thermochimica Acta 417, 301-309.
Ghanem Nevine, B., 2011. Study on the antimicrobial activity of honey products and some Saudi Folkloric substances. Research Journal of Biotechnology 6, 38-43.
Gherman, T., Popescu, V., Carpa, R., Gavril, G.L., Rapa, M., Oprescu, E.E., 2018. Salvia Officinalis Essential Oil Loaded Gelatin Hydrogel as Potential Antibacterial Wound Dressing Materials. Revista De Chimie 69, 410-414.
Han, J., Lei, T., Wu, Q., 2013. Facile preparation of mouldable polyvinyl alcohol-borax hydrogels reinforced by well-dispersed cellulose nanoparticles: physical, viscoelastic and mechanical properties. Cellulose 20, 2947-2958.
Han, J., Lei, T., Wu, Q., 2014. High-water-content mouldable polyvinyl alcohol-borax hydrogels reinforced by well-dispersed cellulose nanoparticles: Dynamic rheological properties and hydrogel formation mechanism. Carbohydrate Polymers 102, 306-316.
Hromiš, N.M., Lazić, V.L., Markov, S.L., Vaštag, Ž.G., Popović, S.Z., Šuput, D.Z., Džinić, N.R., Velićanski, A.S., Popović, L.M., 2015. Optimization of chitosan biofilm properties by addition of caraway essential oil and beeswax. Journal of Food Engineering 158, 86-93.
Huang, X., Brazel, C.S., 2001. On the importance and mechanisms of burst release in matrix-controlled drug delivery systems. Journal of Controlled Release 73, 121-136.
Hussein, Y., Loutfy, S.A., Kamoun, E.A., El-Moslamy, S.H., Radwan, E.M., Elbehairi, S.E.I., 2021. Enhanced anti-cancer activity by localized delivery of curcumin form PVA/CNCs

hydrogel membranes: Preparation and in vitro bioevaluation. International Journal of Biological Macromolecules 170, 107-122.
Jaiswal, M., Gupta, A., Agrawal, A.K., Jassal, M., Dinda, A.K., Koul, V.J.J.o.b.n., 2013. Bi-layer composite dressing of gelatin nanofibrous mat and poly vinyl alcohol hydrogel for drug delivery and wound healing application: in-vitro and in-vivo studies. Journal of Biomedical Nanotechnology 9, 1495-1508.
Kang, J.I., Park, K.M., 2021. Advances in gelatin-based hydrogels for wound management. Journal of Materials Chemistry B 9, 1503-1520.
Konstantinov, A., Vladimirov, G., Grigoryev, A., Kudryavtsev, A., Perminova, I., Nikolaev, E., 2013. Molecular composition study of Mumijo from different geographic areas using size-exclusion chromatography, NMR spectroscopy, and high-resolution mass spectrometry, Functions of Natural Organic Matter in Changing Environment. Springer, pp. 283-287.
L. Cacicedo, M., E. León, I., S. Gonzalez, J., M. Porto, L., A. Alvarez, V., Castro, G.R., 2016. Modified bacterial cellulose scaffolds for localized doxorubicin release in human colorectal HT-29 cells. Colloids and Surfaces B: Biointerfaces 140, 421-429.
Li, Y.-q., Kong, D.-x., Wu, H., 2013. Analysis and evaluation of essential oil components of cinnamon barks using GC–MS and FTIR spectroscopy. Industrial Crops and Products 41, 269-278.
Liu, J., Wang, S., Xu, K., Fan, Z., Wang, P., Xu, Z., Ren, X., Hu, S., Gao, Z., 2020. Fabrication of double crosslinked chitosan/gelatin membranes with Na+ and pH dual-responsive controlled permeability. %J Carbohydrate Polymers 236, 115963.
Liu, Y., Ng, S.C., Yu, J., Tsai, W.-B., 2019. Modification and crosslinking of gelatin-based biomaterials as tissue adhesives. Colloids Surfaces B: Biointerfaces 174, 316-323.
Maitra, J., Shukla, V.K., 2014. Cross-linking in hydrogels-a review. American Journal of Polymer Science 4, 25-31.
Miguel, M.G., 2010. Antioxidant and anti-inflammatory activities of essential oils: a short review. Molecules 15, 9252-9287.
Ngamekaue, N., Chitprasert, P., 2019. Effects of beeswax-carboxymethyl cellulose composite coating on shelf-life stability and intestinal delivery of holy basil essential oil-loaded gelatin microcapsules. International Journal of Biological Macromolecules 135, 1088-1097.
Ngwabebhoh, F.A., Patwa, R., Zandraa, O., Saha, N., Saha, P., 2021. Preparation and characterization of injectable self-antibacterial gelatin/carrageenan/bacterial cellulose hydrogel scaffolds for wound healing application. Journal of Drug Delivery Science and Technology 63, 102415.
Ngwabebhoh, F.A., Yildiz, U., 2019. Nature-derived fibrous nanomaterial toward biomedicine and environmental remediation: Today's state and future prospects. Journal of Applied Polymer Science 136, 47878.
Nikkhah, M., Akbari, M., Paul, A., Memic, A., Dolatshahi-Pirouz, A., Khademhosseini, A., 2016. Gelatin-Based Biomaterials For Tissue Engineering And Stem Cell Bioengineering. Biomaterials from Nature for Advanced Devices Therapies, 37-62.
Pandey, M., Mohamad, N., Amin, M.C.I.M., 2014. Bacterial cellulose/acrylamide pH-sensitive smart hydrogel: development, characterization, and toxicity studies in ICR mice model. Molecular pharmaceutics 11, 3596-3608.
Patwa, R., Saha, N., Sáha, P., 2020a. Magnetic hydrogel based shoe insoles for prevention of diabetic foot. Journal of Magnetism Magnetic Materials 514, 167153.

Patwa, R., Zandraa, O., Capáková, Z., Saha, N., Sáha, P., 2020b. Effect of Iron-Oxide Nanoparticles Impregnated Bacterial Cellulose on Overall Properties of Alginate/Casein Hydrogels: Potential Injectable Biomaterial for Wound Healing Applications. Polymers 12, 2690.

Rehan, I., Muhammad, R., Rehan, K., Karim, K., Sultana, S., 2017. Quantitative analysis of Shilajit using laser-induced breakdown spectroscopy and inductively coupled plasma/optical emission spectroscopy. Journal of Nutrition & Food Sciences 7, 1-9.

Schmitt, S., Schaefer, U., Sporer, F., Reichling, J., 2010. Comparative study on the in vitro human skin permeation of monoterpenes and phenylpropanoids applied in rose oil and in form of neat single compounds. Die Pharmazie-An International Journal of Pharmaceutical Sciences 65, 102-105.

Shah, R., Stodulka, P., Skopalova, K., Saha, P., 2019. Dual crosslinked collagen/chitosan film for potential biomedical applications. Polymers 11, 2094.

Shahrokhi, N., Keshavarzi, Z., Khaksari, M., 2015. Ulcer healing activity of Mumijo aqueous extract against acetic acid induced gastric ulcer in rats. Journal of Pharmacy Bioallied Sciences 7, 56.

Shamloo, A., Aghababaie, Z., Afjoul, H., Jami, M., Bidgoli, M.R., Vossoughi, M., Ramazani, A., Kamyabhesari, K., 2021. Fabrication and evaluation of chitosan/gelatin/PVA hydrogel incorporating honey for wound healing applications: An in vitro, in vivo study. International Journal of Pharmaceutics 592, 120068.

Shimizu, N., Ishida, D., Yamamoto, A., Kuroyanagi, M., Kuroyanagi, Y., 2014. Development of a functional wound dressing composed of hyaluronic acid spongy sheet containing bioactive components: evaluation of wound healing potential in animal tests. Journal of Biomaterials Science, Polymer Edition 25, 1278-1291.

Špaldoňová, A., Havelcová, M., Lapčák, L., Machovič, V., Titěra, D., 2020. Analysis of beeswax adulteration with paraffin using GC/MS, FTIR-ATR and Raman spectroscopy. Journal of Apicultural Research, 1-11.

Spoljaric, S., Salminen, A., Luong, N.D., Seppälä, J., 2014. Stable, self-healing hydrogels from nanofibrillated cellulose, poly(vinyl alcohol) and borax via reversible crosslinking. European Polymer Journal 56, 105-117.

Stohs, S.J., Singh, K., Das, A., Roy, S., Sen, C.K., 2017. Energy and Health Benefits of Shilajit, Sustained Energy for Enhanced Human Functions and Activity. Elsevier, pp. 187-204.

Sukhdolgor, J., Orkhonselenge, D., 2011. Biochemical Study of Mumijo in Uvs province, Mongolia. Mongolian Journal of Chemistry 12, 56-59.

Szulc, J., Machnowski, W., Kowalska, S., Jachowicz, A., Ruman, T., Steglińska, A., Gutarowska, B., 2020. Beeswax-Modified Textiles: Method of Preparation and Assessment of Antimicrobial Properties. Polymers 12, 344.

Talbert, R., Hartman, M., Schepetkin, I.A., Xie, G., Jutila, M.A., Dhungana, R., Subedi, R., 2014. Mumijo Traditional Medicine. Complement.

Tanner, N., Lichtenberg-Kraag, B., 2019. Identification and Quantification of Single and Multi-Adulteration of Beeswax by FTIR-ATR Spectroscopy. European Journal of Lipid Science Technology 121, 1900245.

Tao, G., Wang, Y., Cai, R., Chang, H., Song, K., Zuo, H., Zhao, P., Xia, Q., He, H., 2019. Design and performance of sericin/poly (vinyl alcohol) hydrogel as a drug delivery carrier for potential wound dressing application. Materials Science Engineering: C 101, 341-351.

Tayeb, A.H., Amini, E., Ghasemi, S., Tajvidi, M., 2018. Cellulose nanomaterials—Binding properties and applications: A review. Molecules 23, 2684.

Treesuppharat, W., Rojanapanthu, P., Siangsanoh, C., Manuspiya, H., Ummartyotin, S., 2017. Synthesis and characterization of bacterial cellulose and gelatin-based hydrogel composites for drug-delivery systems. Biotechnology Reports 15, 84-91.

Tsai, M.-L., Lin, C.-C., Lin, W.-C., Yang, C.-H., 2011. Antimicrobial, antioxidant, and anti-inflammatory activities of essential oils from five selected herbs. Bioscience, Biotechnology, and Biochemistry, 1108312632-1108312632.

Vargas, G., Acevedo, J.L., López, J., Romero, J., 2008. Study of cross-linking of gelatin by ethylene glycol diglycidyl ether. Materials Letters 62, 3656-3658.

Voidarou, C., Alexopoulos, A., Plessas, S., Karapanou, A., Mantzourani, I., Stavropoulou, E., Fotou, K., Tzora, A., Skoufos, I., Bezirtzoglou, E., 2011. Antibacterial activity of different honeys against pathogenic bacteria. Anaerobe 17, 375-379.

Yang, C., Xu, L., Zhou, Y., Zhang, X., Huang, X., Wang, M., Han, Y., Zhai, M., Wei, S., Li, J., 2010. A green fabrication approach of gelatin/CM-chitosan hybrid hydrogel for wound healing. Carbohydrate Polymers 82, 1297-1305.

Zandraa, O., Jelínková, L., Roy, N., Sáha, T., Kitano, T., Saha, N., 2011. Viscoelastic properties and morphology of mumio-based medicated hydrogels, AIP Conference Proceedings. American Institute of Physics, pp. 261-271.

Zheng, Y., Liang, Y., Zhang, D., Sun, X., Liang, L., Li, J., Liu, Y.-N., 2018. Gelatin-based hydrogels blended with gellan as an injectable wound dressing. ACS omega 3, 4766-4775.